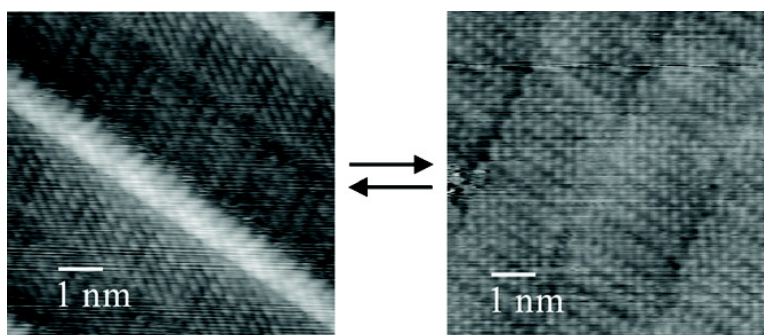


Phase Transition of a Single Sheet of Sashlike Polydiacetylene Atomic Sash on a Solid Surface

Osamu Endo, Hiroaki Ootsubo, Naoya Toda, Masanori Suhara, Hiroyuki Ozaki, and Yasuhiro Mazaki

J. Am. Chem. Soc., **2004**, 126 (32), 9894-9895 • DOI: 10.1021/ja047841g • Publication Date (Web): 23 July 2004

Downloaded from <http://pubs.acs.org> on April 1, 2009



More About This Article

Additional resources and features associated with this article are available within the HTML version:

- Supporting Information
- Links to the 2 articles that cite this article, as of the time of this article download
- Access to high resolution figures
- Links to articles and content related to this article
- Copyright permission to reproduce figures and/or text from this article

[View the Full Text HTML](#)

Phase Transition of a Single Sheet of Sashlike Polydiacetylene Atomic Sash on a Solid Surface

Osamu Endo,[†] Hiroaki Ootsubo,[†] Naoya Toda,[†] Masanori Suhara,[†] Hiroyuki Ozaki,^{*,†} and Yasuhiro Mazaki[‡]

Department of Organic and Polymer Materials Chemistry, Faculty of Technology, Tokyo University of Agriculture and Technology, Koganei, Tokyo 184-8588, Japan, and Department of Chemistry, School of Science, Kitasato University, Sagamihara, Kanagawa 228-8555, Japan

Received April 15, 2004; E-mail: hiroyuki@cc.tuat.ac.jp

The chromatic transition (from blue to red or vice versa) of polydiacetylenes (PDs) has been studied widely for many years.¹ The transition can be induced thermally, optically, mechanically, and chemically and is therefore expected to open a new application field, including optoelectronics and biosensors.² The structural analyses by Raman spectroscopy,³ NMR,⁴ and X-ray diffraction⁵ revealed that the strength of C–C, C=C, and C≡C bonds in the PD chains, the conformation of methylenes in the side groups, and the effective conjugation length change upon transition. We have tried to obtain the minute picture of such a phenomenon in an extrathin (0.4 nm) PD monolayer by scanning tunneling microscopy (STM), which has become a powerful tool for observing the real space images of organic molecules in various monolayers.⁶ We demonstrate here that variable-temperature STM under ultrahigh vacuum (UHV) enables us to observe two interconvertible phases of PD in a monolayer of sashlike polymer *atomic sash* (AS) on a graphite (0001) surface.

We reported electron spectroscopic studies on AS monolayers prepared by the photopolymerization of 17,19-hexatriacontadiyne (HTDY) molecules laid flat and packed closely on graphite.^{7,8} The internal structure of AS and the column or lamella structures in the monomer monolayer deduced from the van der Waals packing of HTDY and the polymerization conditions^{7,8} were confirmed by STM in the air.⁹ On the other hand, a different structural model was proposed for PD monolayers prepared by the light- and tip-induced polymerization of diacetylene derivatives at air/solid interfaces.^{10–12} In this study, we have obtained a clue to the origin of the discrepancy.

Film preparation and STM observation were carried out with a UHV apparatus reported previously.¹³ A piece of highly oriented pyrolytic graphite (HOPG) cleaved in the air was degassed at 650 K under UHV for 24 h. HTDY was deposited onto the graphite (0001) surface at room temperature (rt) to obtain a uniform monolayer of column structure with flat-on orientation.¹³ The molecules were polymerized by UV irradiation from a deuterium lamp at 220 K or at rt.^{7,8}

Figure 1 shows STM images for successive stages during the monolayer polymerization of HTDY and the phase transition of AS. In the image of an unirradiated HTDY monolayer (a), we can observe an array of bright lines; the 5 nm spacing corresponds to the width of each column of flat-on molecules (see the inset), and the bright lines can be related to the diacetylene moiety of HTDY around which the LUMO is distributed.^{9,13} By UV irradiation, lines with high contrast appear and the number increases with time (b and c). These lines are ascribable to AS-I with raised PD chains (see Figure 2c and discussion below). After almost all low-contrast

lines due to diacetylene columns change to high-contrast lines and the monolayer is maintained at rt or irradiated further (or else an HTDY monolayer is irradiated for shorter time at rt from the beginning), parts of them lose contrast (d). The pale regions are attributed to AS-II with a planar structure^{7–9} (see Figure 2d). Finally, remaining sashes I are transformed into sashes II, and features due to the array of PD chains are missing (Figure 1e). After an AS-II monolayer such as the film in Figure 1e is maintained at 80 K over 3 days, sashes II are transformed back into sashes I (f), although the PD chains seem broken in places.

A small-scale STM image of an AS-I monolayer, corresponding to the large-scale image in Figure 1c, is shown in Figure 2a. The PD chains exhibit high contrast as wide as 1 nm, suggesting that MOs responsible for the image have a large electron distribution at the α -methylene units also. The alkyl chains are arranged perpendicularly to the PD chains. The structural model in Figure 2c is constructed so that the high contrast for the middle of the sashes reflects the geometrical height. As shown in the cross section, the PD chains are raised by rotated methylenes at the β - and γ -carbon atoms of the alkyl chains in both sides. The structure is in accordance with the model by Okawa et al.¹¹ We point out here that it represents a structural feature characteristic of the low-temperature phase (LP) of bulk PD having methylenes directly combined to the PD chain:^{3,4} the β - γ -methylenes are in gauche conformation. Furthermore, it is the LP that is obtained first from the diacetylene monomer in general.^{1–5} Miura et al. also reported that PD chains maintained at positions higher than the alkyl chains are formed by the polymerization of the monolayer of diacetylene derivatives containing alkyl chains.¹² The effective conjugation length seems to be considerably large (more than 250 nm or ca. 500 repeat units) for AS-I in Figure 1c, which is also consistent with the characteristic of the LP of most PDs.^{1–5} Thus, we conclude that Figure 2a exhibits AS-I in the LP. Though the resolution for the rest of the alkyl chains is not perfect and every two methylene units are seen combined, the direction of the pairs is not perpendicular to that of the alkyl chains, in line with the flat-on orientation of the alkyl chains except at α - and β -positions^{14,16} (see Supporting Information for the conformation at the α - β -methylenes and the alkyl chain direction).

A small-scale STM image for an AS-II monolayer such as the film in Figure 1e is shown in Figure 2b. The PD chains are rather darker than other parts in contrast to the bright diacetylene columns of the HTDY monolayer in Figure 1a, which cannot be explained by the simple ionization potential (or electron affinity) model^{14,15} because the energy of the HOMO (or LUMO) is raised (or lowered) upon polymerization. It may be due to different tunneling mechanism for the semiconducting polymer. Fine structures in this image represent the positions of the hydrogen atoms of methylenes as in

[†] Tokyo University of Agriculture and Technology.

[‡] Kitasato University.

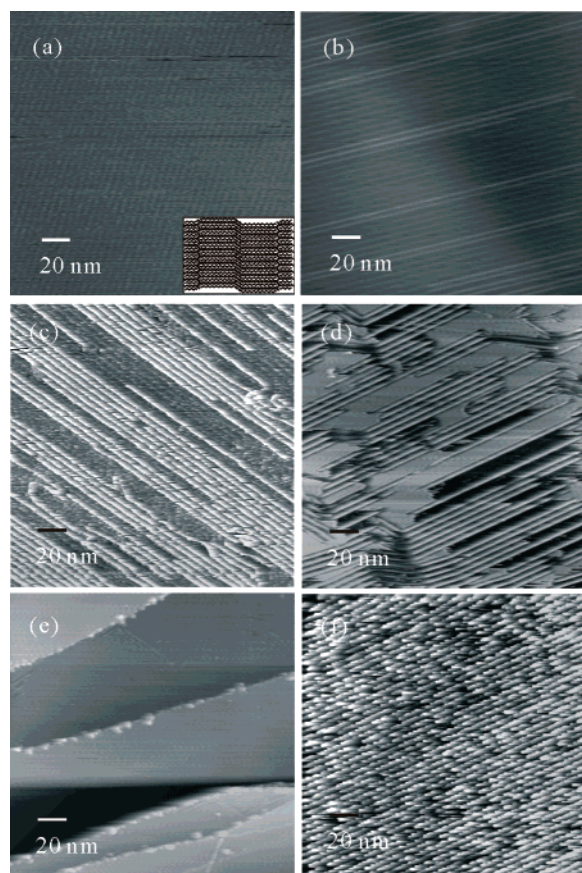


Figure 1. Large-scale STM images ($200 \times 200 \text{ nm}^2$) for successive stages during the monolayer polymerization of HTDY and the phase transition of AS. (a) Unirradiated HTDY monolayer prepared by vapor deposition on graphite (0001) at room temperature (rt); observed at rt with sample bias voltage $V = 2.00 \text{ V}$ and tunneling current $I = 80 \text{ pA}$. (b and c) Partially polymerized monolayer after irradiating an HTDY monolayer with UV light at 220 K for 1 h (b) and 10 h (c); observed at 200 K, $V = 1.00 \text{ V}$, $I = 70 \text{ pA}$ (b) and at 140 K, $V = -2.00 \text{ V}$, $I = 80 \text{ pA}$ (c). High-contrast lines correspond to AS-I in the low-temperature phase (LP). (d) Polymer monolayer comprising AS-II in the high-temperature phase (HP) (pale regions) as well as AS-I, obtained by irradiating an HTDY monolayer at rt for 3 h; observed at rt, $V = -1.00 \text{ V}$, $I = 15 \text{ pA}$. Black regions represent polymers in intermediate states between AS-I and AS-II (see Supporting Information). (e) AS-II monolayer obtained by maintaining a film (d) at rt for 15 h; observed at rt, $V = -1.00 \text{ V}$, $I = 20 \text{ pA}$. (f) AS-I monolayer obtained by cooling an AS-II monolayer such as the film in e at 80 K over 3 days; observed at 80 K, $V = -2.20 \text{ V}$, $I = 80 \text{ pA}$.

the cases of *n*-alkane monolayers.^{14,16} The direction of the alkyl chains is inclined about 75° against the PD chains. This image essentially agrees with that obtained in the air and our structural model shown in Figure 2d.^{7–9} The alkyl chains are laid flat in all-trans conformation. Since the all-trans conformation and the short conjugation length displayed in Figure 2b¹⁷ are structural features of the high-temperature phase (HP) of bulk PD,^{1–5} AS-II can be regarded as being in the HP. It is also noteworthy that the HP-AS is obtained not by polymerization in the HTDY monolayer directly but by transition from the LP-AS, analogous to the polymerization process of most bulk PDs.^{1–5} In addition, the shortened HP-AS in Figure 1e or 2b can be changed to the LP-AS as in Figure 1f by cooling.

In summary, the monolayer of the sashlike PD atomic sash on graphite (0001) exhibits two interconvertible phases, in which the conformation is different around the crossing points of the alkyl and PD chains, and hence the contrast of the STM image is different in the middle of the sashes. The conjugation length changes upon the transition.

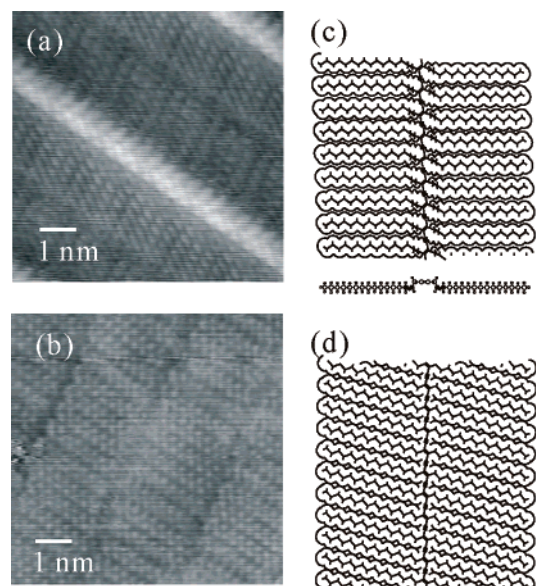


Figure 2. Small-scale STM images ($7.5 \times 7.5 \text{ nm}^2$) of an AS-I monolayer in the LP at 130 K ($V = 2.00 \text{ V}$, $I = 80 \text{ pA}$) (a) and an AS-II monolayer in the HP at 150 K ($V = 2.00 \text{ V}$, $I = 130 \text{ pA}$) (b) together with the corresponding structural models (c and d).

Supporting Information Available: Magnified STM images of Figures 1d, 2a, and 2b with structural models (pdf). This material is available free of charge via the Internet at <http://pubs.acs.org>.

References

- (1) (a) Wegner, G. *Makromol. Chem.* **1971**, *145*, 85–94. (b) *Polydiacetylenes*; Bloor, D.; Chance, R. R., Eds.; Nijhoff: Dordrecht, 1985.
- (2) (a) Charych, D. H.; Nagy, J. O.; Spevak, W.; Bednarski, M. D. *Science* **1993**, *261*, 585–588. (b) Kim, T.; Chan, K. C.; Crooks, R. M. *J. Am. Chem. Soc.* **1997**, *119*, 189–193. (c) Menzel, H.; Mowery, M. D.; Cai, M.; Evans, C. E. *J. Phys. Chem. B* **1998**, *102*, 9550–9556. (d) Cheng, Q.; Stevens, R. C. *Langmuir* **1998**, *14*, 1974–1976.
- (3) Koshihara, S.; Tokura, Y.; Takeda, K.; Koda, T. *Phys. Rev. Lett.* **1992**, *68*, 1148–1151.
- (4) Tanaka, H.; Gomez, M. A.; Tonelli, A. E.; Thakur, M. *Macromolecules* **1989**, *22*, 1208–1215 and 2427–2432.
- (5) Fischetti, R.; Filipkowski, M.; Garito, A. F.; Blasie, J. K. *Phys. Rev. B* **1988**, *37*, 4714–4726.
- (6) (a) Frommer, J. *Angew. Chem., Int. Ed. Engl.* **1992**, *31*, 1298–1328. (b) Smith, D.; Hörber, J.; Binnig, G.; Nejh, H. *Nature* **1990**, *344*, 641–644. (c) Rabe, J. P.; Buchholz, S. *Science* **1991**, *253*, 424–427. (d) Yeo, Y. H.; McGonigal, G. C.; Thomson, D. J. *Langmuir* **1993**, *9*, 649–651. (e) Taki, S.; Ishida, K.; Okabe, H.; Matsushige, K. *J. Cryst. Growth* **1993**, *131*, 13–16. (f) Liang, W.; Whangbo, M.-H.; Wawkuszewski, A.; Cantow, H.-J.; Magonov, S. N. *Adv. Mater.* **1993**, *5*, 817–821. (g) Hibino, M.; Sumi, A.; Hata, I. *Jpn. J. Appl. Phys.* **1995**, *34*, 610–614. (h) Giancarlo, L. C.; Fang, H.; Rubin, S. M.; Bront, A. A.; Flynn, G. W. *J. Phys. Chem. B* **1998**, *102*, 10255–10263. (i) Poulenec, C. L.; Cousty, J.; Xie, Z. X.; Mioskowski, C. *Surf. Sci.* **2000**, *448*, 93–100. (j) Lee, H. S.; Iyengar, S.; Musselman, I. H. *Anal. Chem.* **2001**, *73*, 5532–5538.
- (7) Ozaki, H.; Funaki, T.; Mazaki, Y.; Masuda, S.; Harada, Y. *J. Am. Chem. Soc.* **1995**, *117*, 5596–5597.
- (8) Ozaki, H. *J. Electron Spectrosc. Relat. Phenom.* **1995**, *76*, 377–382.
- (9) Irie, S.; Isoda, S.; Kobayashi, T.; Ozaki, H.; Mazaki, Y. *Probe Microsc.* **2000**, *2*, 1–9.
- (10) Grim, P. C. M.; Feyter, S. D.; Gesquière, A.; Vanoppen, P.; Rücker, M.; Valiyaveetil, S.; Moessner, G.; Müllen, K.; Schryver, F. C. D. *Angew. Chem., Int. Ed. Engl.* **1997**, *36*, 2601–2603.
- (11) Okawa, Y.; Aono, M. *Nature* **2001**, *409*, 683–684.
- (12) Miura, A.; Feyter, S. D.; Abdel-Mottaleb, M. M. S.; Gesquière, A.; Grim, P. C. M.; Moessner, G.; Sieffert, M.; Klapper, M.; Müllen, K.; Schryver, F. C. D. *Langmuir* **2003**, *19*, 6474–6482.
- (13) Endo, O.; Toda, N.; Ozaki, H.; Mazaki, Y. *Surf. Sci.* **2003**, *545*, 41–46.
- (14) Claypool, L.; Faglioni, F.; Goddard, W. A., III; Gray, H. B.; Lewis, N. S.; Marcus, R. A. *J. Phys. Chem. B* **1997**, *101*, 5978–5995.
- (15) Faglioni, F.; Claypool, L.; Lewis, N. S.; Goddard, W. A., III. *J. Phys. Chem. B* **1997**, *101*, 5996–6020.
- (16) Claypool, L.; Faglioni, F.; Goddard, W. A., III; Lewis, N. S.; Marcus, R. A. *J. Phys. Chem. B* **1999**, *103*, 7077–7080.
- (17) Since each AS-II in Figure 2b comprises ca. 6 repeat units (see Supporting Information), it may be more appropriately referred to as oligodiacytylene rather than PD.

JA047841G